

Supporting Information

Mg/Zn Metal-Air Primary Batteries Using Silk Fibroin-Ionic Liquid Polymer Electrolytes.

Mathew J. Haskew, Shahin Nikman, Carys E. O'Sullivan, Hanaa A. Galeb, Nathan R. Halcovitch, John G. Hardy and Samuel T. Murphy**

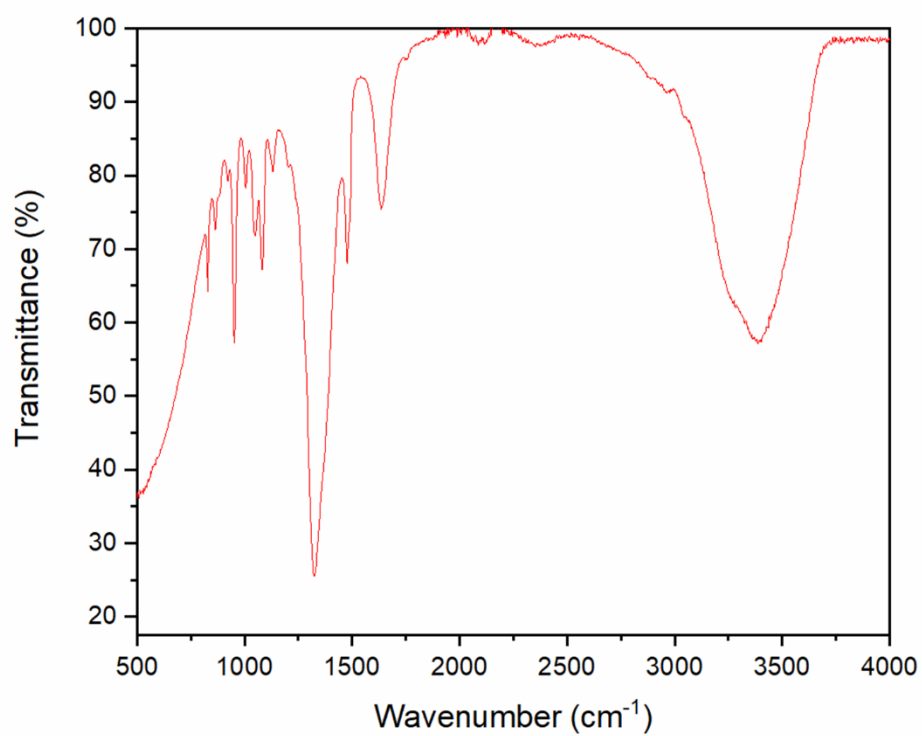


Figure S1. FTIR spectrum of the ionic liquid choline nitrate [Ch][NO₃]. Strong bands at 1330 cm⁻¹ for vibrations of NO₃⁻ and 954 cm⁻¹ for vibrations of C-C-OH, characteristic of the IL.

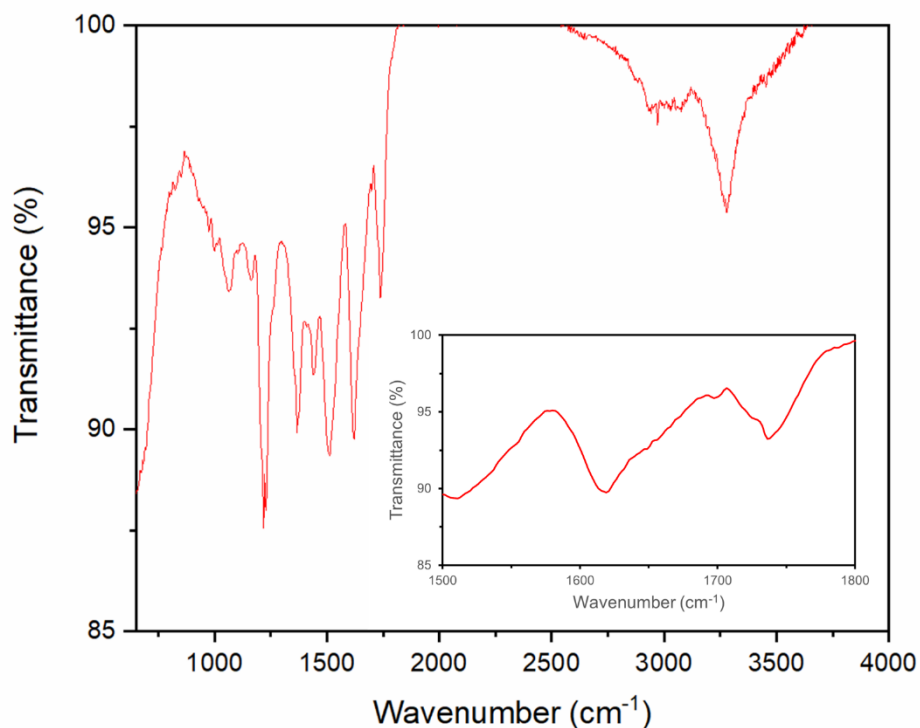


Figure S2. FTIR spectrum of the *B. mori* SF film. Peaks observed at ca. 1690 cm⁻¹ amide I (characteristic of β -turns), 1625 cm⁻¹ amide I (characteristic of β -sheets), ca. 1550 cm⁻¹ amide II (unordered), 1520 cm⁻¹ Tyr-OH, ca. 1510 cm⁻¹ amide II (β -sheets), ca. 1313 cm⁻¹ amide III (β -turns), ca. 1219 cm⁻¹ amide III (β -sheets), characteristic of *B. mori* SF.

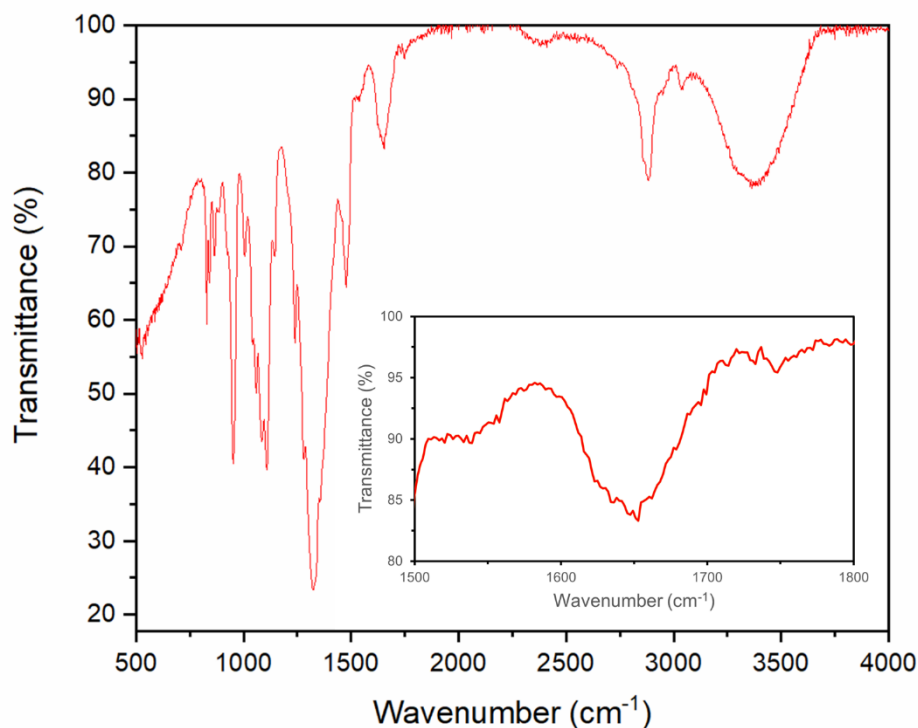


Figure S3. FTIR spectrum of the 1:1 wt ratio of SF:IL PE film. The absorbance bands characteristic of the IL are clearly observed at 1330 cm^{-1} for vibrations of NO_3^- and 954 cm^{-1} for vibrations of C-C-OH. Peaks observed at ca. 1690 cm^{-1} amide I (characteristic of β -turns), 1625 cm^{-1} amide I (characteristic of β -sheets), ca. 1550 cm^{-1} amide II (unordered), 1520 cm^{-1} Tyr-OH, ca. 1510 cm^{-1} amide II (β -sheets), ca. 1313 cm^{-1} amide III (β -turns), ca. 1219 cm^{-1} amide III (β -sheets), characteristic of *B. mori* SF.

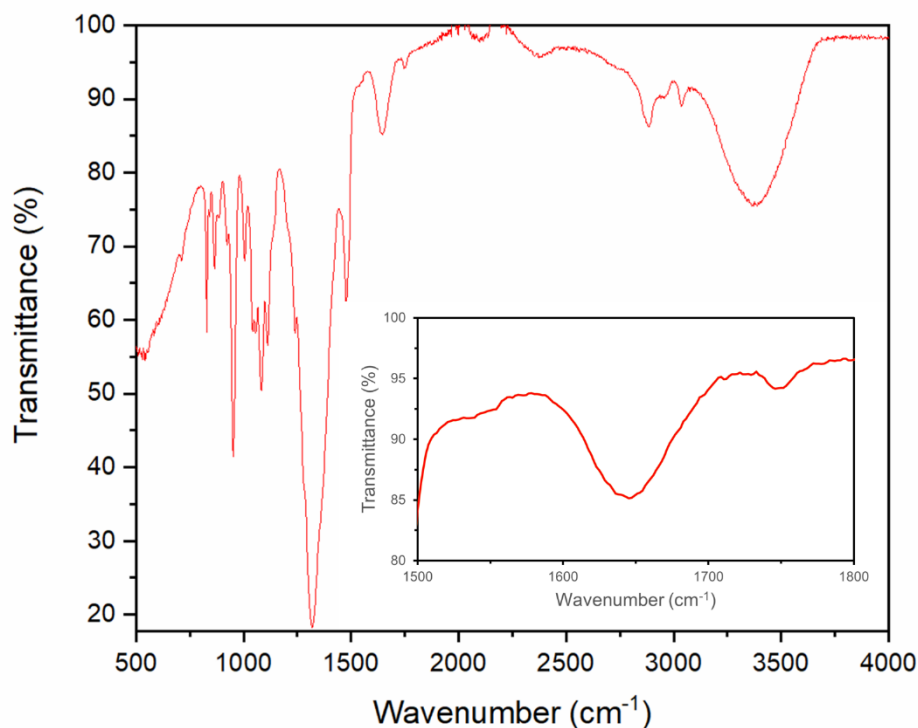


Figure S4. FTIR spectrum of the 1:3 wt ratio of SF:IL PE film. The absorbance bands characteristic of the IL are observed at 1330 cm^{-1} for vibrations of NO_3^- and 954 cm^{-1} for vibrations of C-C-OH. Peaks observed at ca. 1690 cm^{-1} amide I (characteristic of β -turns), 1625 cm^{-1} amide I (characteristic of β -sheets), ca. 1550 cm^{-1} amide II (unordered), 1520 cm^{-1} Tyr-OH, ca. 1510 cm^{-1} amide II (β -sheets), ca. 1313 cm^{-1} amide III (β -turns), ca. 1219 cm^{-1} amide III (β -sheets), characteristic of *B. mori* SF.

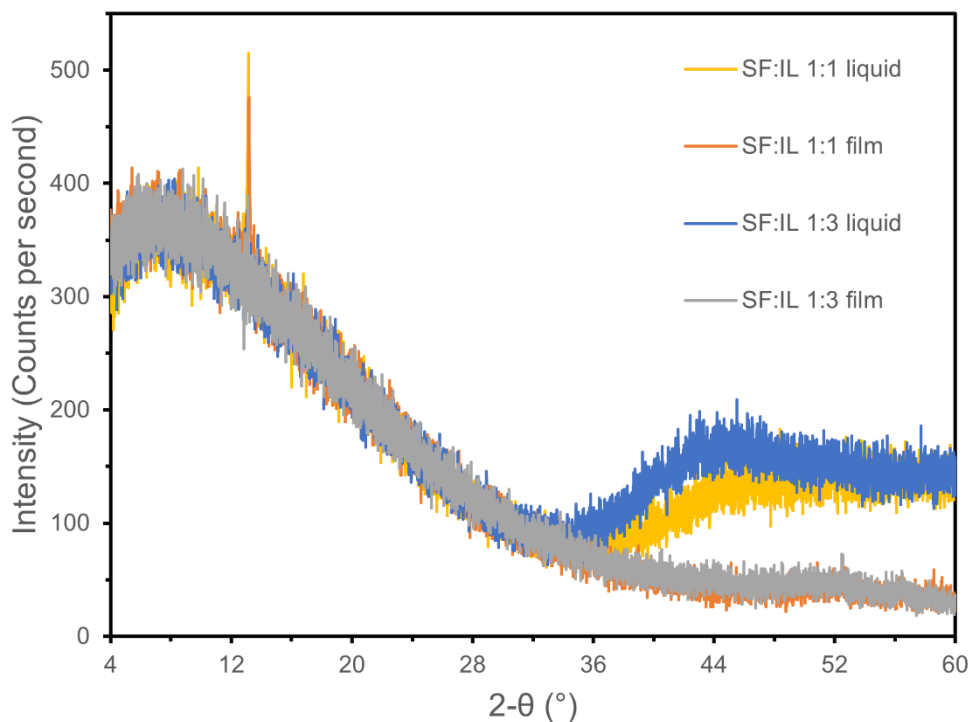


Figure S5. XRD of the materials studied herein. **Yellow line)** 1:1 SF:IL PE in the solution/liquid state: the diffractogram indicates a broad peak at ca. 8° $2\text{-}\theta$ (amorphous, silk I) and a peak at ca. 13° $2\text{-}\theta$ (β -turn, silk I). **Orange line)** XRD of the 1:1 SF:IL PE in the solid (film) state: the diffractogram indicates a broad peak at ca. 8° $2\text{-}\theta$ (amorphous, silk I) and a peak at ca. 13° $2\text{-}\theta$ (β -turn, silk I). **Blue line)** XRD of the 1:3 SF:IL PE in the solution/liquid state. The diffractogram indicates a broad peak at ca. 8° $2\text{-}\theta$ (amorphous, silk I). **Grey line)** XRD of the 1:3 SF:IL PE in the solid (film) state: the diffractogram indicates a broad peak at ca. 8° $2\text{-}\theta$ (amorphous, silk I).

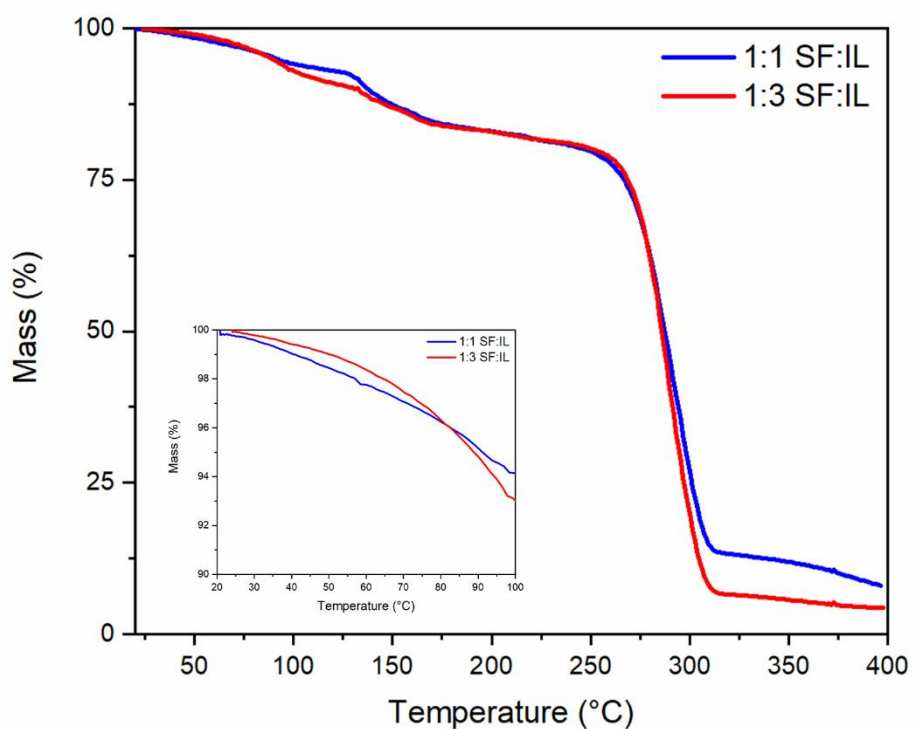


Figure S6. TGA curves for the PE 1:1 and 1:3 films. Average of 3 measurements. The heating was conducted under a nitrogen atmosphere at a rate of $5\text{ }^{\circ}\text{C min}^{-1}$. The inset portrays the expanded view (20 to 100 °C) of the averaged TGA curves for PE 1:1 and 1:3, blue and red lines, respectively.

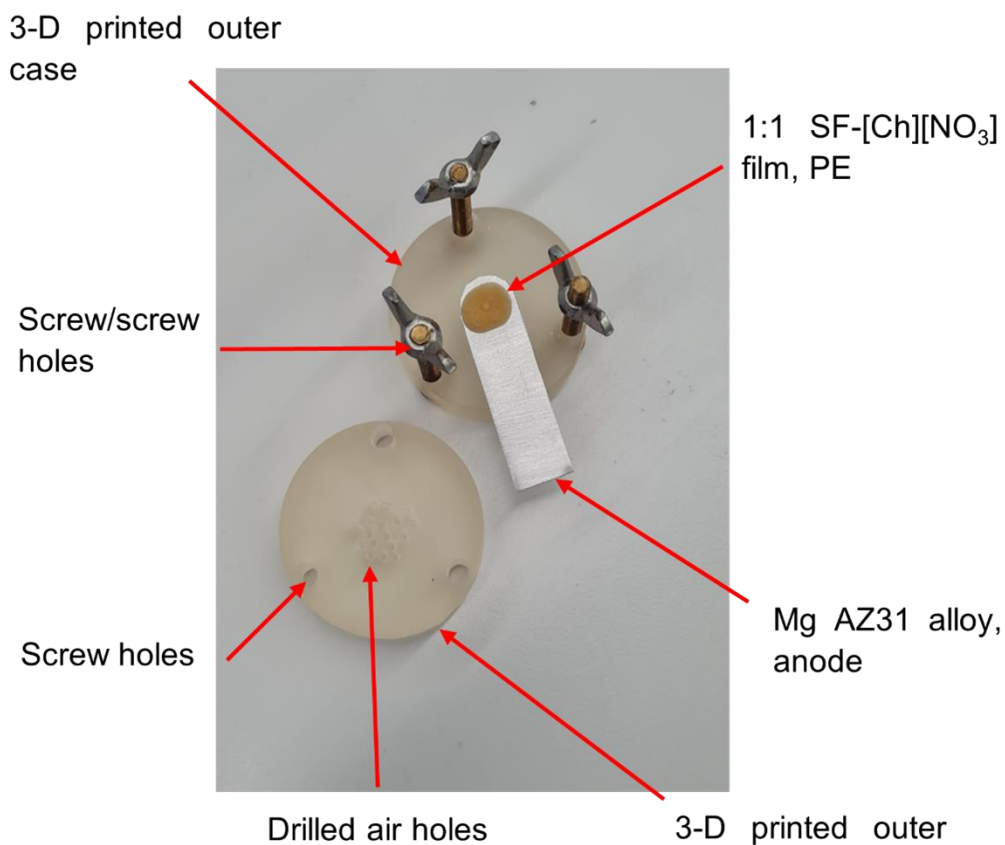


Figure S7. Picture of the 1:1 SF:IL PE film on top of the Mg AZ31 alloy as the anode. Labelled correspondingly by the red arrows. During assembly, areas of the anode foil around the PE film were taped using clear Sellotape, preventing the metal foil and air terminals (anode and cathode) from contacting one another.

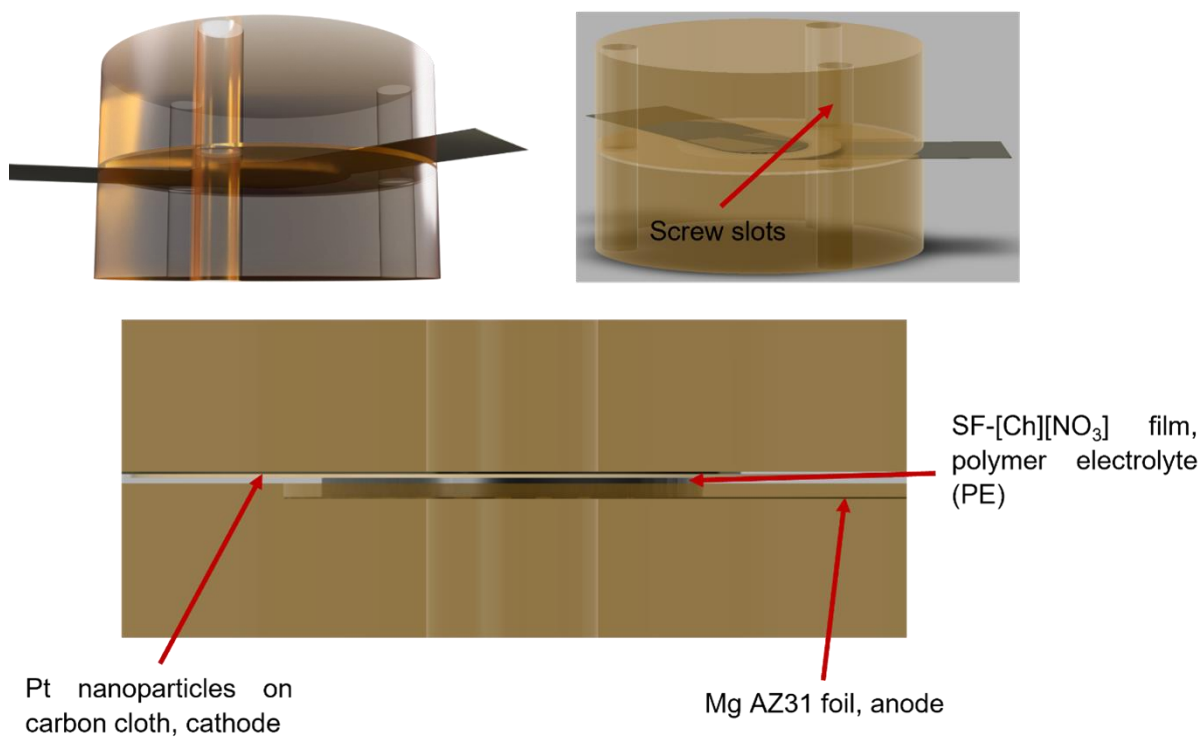


Figure S9. Computer aided design (CAD) illustration of the solid-state metal-air battery. Exemplified with a Mg AZ31 foil anode and Pt nanoparticle coated carbon cloth cathode, labelled correspondingly by the red arrows.

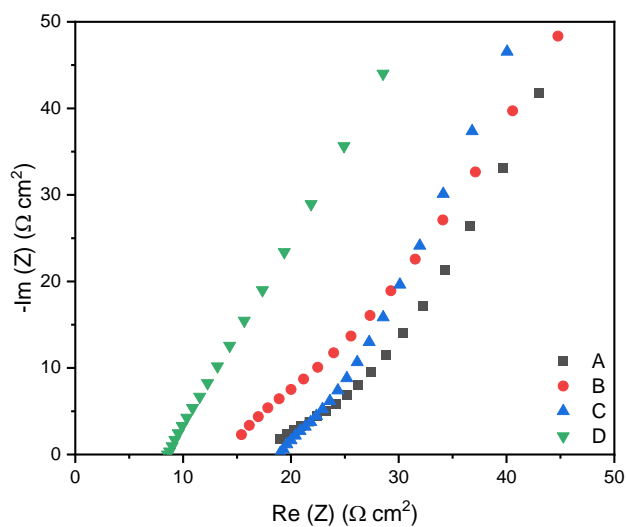


Figure S10. **A)** PEIS spectra of the 1:1 PE assembled in the primary Mg-air battery: expanded view of the high frequency region. **B)** PEIS spectra of the 1:3 PE assembled in the primary Mg-air battery: expanded view of the high frequency region. **C)** PEIS spectra of the 1:1 PE assembled in the primary Zn-air battery: expanded view of the high frequency region. **D)** PEIS spectra of the 1:3 PE assembled in the primary Zn-air battery: expanded view of the high frequency region.

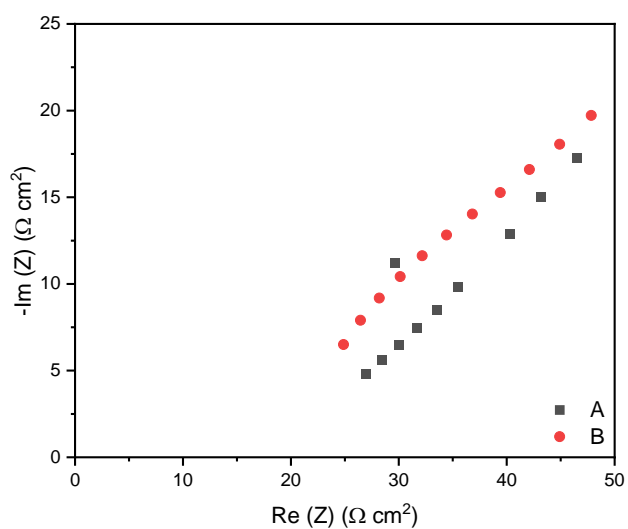


Figure S11. A) PEIS spectra of the 1:1 PE assembled in the primary Mg-air battery post discharge: expanded view of the high frequency region. B) PEIS spectra of the 1:3 PE assembled in the primary Mg-air battery post discharge: expanded view of the high frequency region.

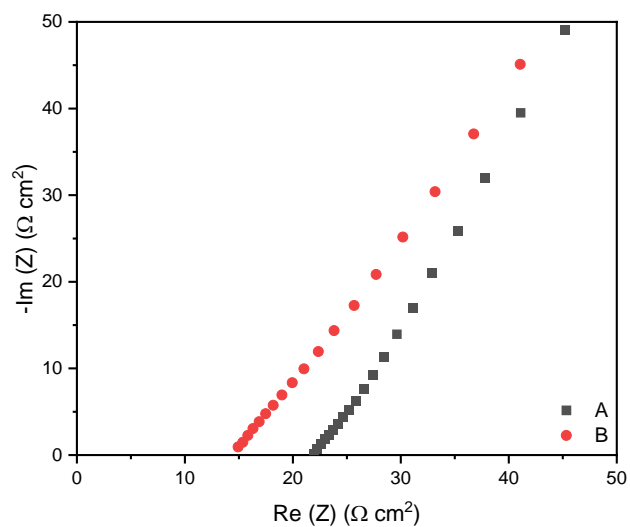


Figure S12. A) PEIS spectra of the 1:1 PE assembled in the primary Zn-air battery post discharge: expanded view of the high frequency region. B) PEIS spectra of the 1:3 PE assembled in the primary Zn-air battery post discharge: expanded view of the high frequency region.

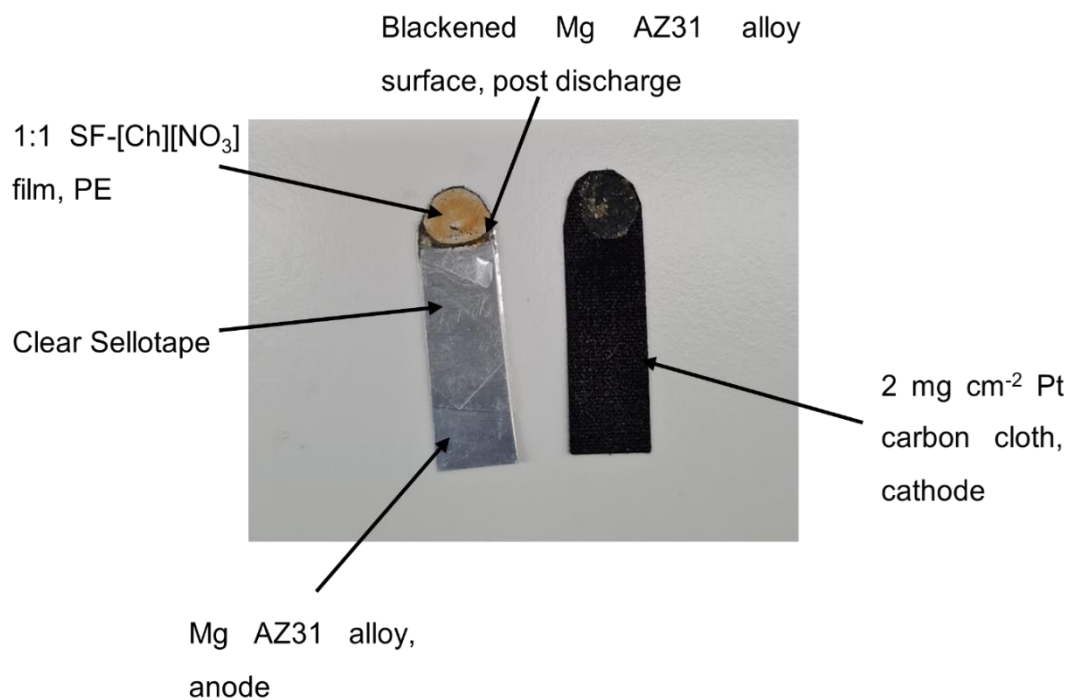


Figure S13. Picture of the Mg AZ31 anode and Pt carbon cloth cathode post discharge. The electrodes were taken from the primary Mg-air battery using the 1:1 SF:IL PE film after discharging at a current density of $25 \mu\text{A cm}^{-2}$.